Journal of Photonics for Energy

PhotonicsforEnergy.SPIEDigitalLibrary.org

Perovskites: transforming photovoltaics, a mini-review

Ashwith Kumar Chilvery
Ashok K. Batra
Bin Yang
Kai Xiao
Padmaja Guggilla
Mohan D. Aggarwal
Raja Surabhi
Ravi B. Lal
James R. Currie
Benjamin G. Penn

SPIE.

REVIEW

Perovskites: transforming photovoltaics, a mini-review

Ashwith Kumar Chilvery,[a,b,*] Ashok K. Batra,[b] Bin Yang,[c] Kai Xiao,[c] Padmaja Guggilla,[b] Mohan D. Aggarwal,[b] Raja Surabhi,[b] Ravi B. Lal,[b] James R. Currie,[d] and Benjamin G. Penn[d]

[a]Talladega College, Department of Physics, 627 West Battle Street, Talladega, Alabama 35610, United States

[b]Alabama A&M University, Material Science Group, Department of Physics, Chemistry and Mathematics, 4900 Meridian Street, Normal, Alabama 35762, United States

[c]Center for Nanophase Material Science, Oak Ridge National Laboratory, Bethel Valley Road, Oak Ridge, Tennessee 37831, United States

[d]NASA-Marshall Space Flight Center, Sensors Group, Redstone Arsenal, Huntsville, Albama 35811, United States

Abstract. The recent power-packed advent of perovskite solar cells is transforming photovoltaics (PV) with their superior efficiencies, ease of fabrication, and cost. This perovskite solar cell further boasts of many unexplored features that can further enhance its PV properties and lead to it being branded as a successful commercial product. This article provides a detailed insight of the organometal halide based perovskite structure, its unique stoichiometric design, and its underlying principles for PV applications. The compatibility of various PV layers and its fabrication methods is also discussed.
[DOI: 10.1117/1.JPE.5.057402]

Keywords: perovskites; charge transport; dielectric; photovoltaics; efficiency.

Paper 14060SS received Sep. 12, 2014; accepted for publication Nov. 14, 2014; published online Jan. 6, 2015.

1 Introduction

Solar energy, an infinite producer of photons with a broad range of wavelengths, continues to be a potential source of clean energy. The photovoltaic (PV) process is considered as an ideal energy conversion process that can meet this requirement.[1] The International Energy Agency's technology roadmap estimates that by 2050, PV will provide ~11% of all global electricity production and avoid 2.3 gigatonnes of CO_2 emissions per year.[2] Given these predictions, photovoltaics or light-to-voltage converting devices have gained unprecedented attention from the research communities in the previous decades. Many researchers believe that solar cells, the basic building block of photovoltaics, are on the verge of creating a big impact by providing sustainable and efficient energy via cost-effective methods.

The Sun's energy can be harnessed in many ways. One example could be of a PV module that converts solar energy into electricity and a solar thermal collector that converts solar energy into heat, such as for domestic hot water or room heating.[3] Hence, exploring ways to realize PV as cheaper, reliable, and durable ways to generate power is of interest to the scientific community. Silicon, the 14th element on the periodic table, is crucial for PV material in today's world. However, there is still a need for newer materials and methodologies that offer better throughputs and efficiencies.[4]

The first generation of the solar cells dates back to 1953, when Gerald Pearson, Daryl Chapin, and Calvin Fuller discovered the silicon solar cell at AT&T Bell Labs.[5] Currently, they trail on the efficiency chart at 25%.[6] The use of polycrystalline silicon, thin films, and

*Address all correspondence to: Ashwith Kumar Chilvery, E-mail: akchilvery@talladega.edu

This review manuscript is also part of the section on "Breakthroughs in Photonics and Energy," highlighting primarily recent advances in the last three years.

0091-3286/2015/$25.00

compound semiconductors rose in the era of second-generation solar cells, which entered the PV market in 1981.[7] Currently, second-generation solar cells top the efficiency chart at 45%.[8] In early 2000, organic solar cells paved way for a third wave of PV technology, which brings the advantages of flexibility, cost-effectiveness, and ease of fabrication. Though silicon-based solar cells continue to dominate over thin-film technologies and are flying high due to impressive efficiencies and better lifetimes, it is still in the interest of mankind to unwrap the organic horizon of solar cells. Therefore, there has been a greater demand in the past decade on scientists to discover flexible, cheaper, mass producible, and lightweight organic solar cells. One possible alternative to address this problem is to develop PV cells from materials that can be processed as easily as plastics. Augmenting this demand, the conferring of the Nobel Prize in Chemistry for the year 2000 to Dr. Alan Heeger in recognition of his work on conducting polymers has decisively paved a new era in the field of organic electronics, organic photovoltaics (OPVs), and organic/flexible displays.[9] This has, in turn, led to the flexible third-generation solar cells, which are organic, dye-sensitized, and polymer. Figure 1 briefly differentiates inorganic solar cells from their organic counterparts.

Organic solar cells (OSC) or plastic solar cells are an evolving multidisciplinary area of research that involve theoretical, experimental, and design challenges dealing with carbon-based materials and other organic compounds.[10] It is a brand of polymer solar cell that incorporates a conductive organic polymer for light absorption, exciton dissociation, and charge transport to generate electricity.[11] The OPVs based on a single conducting polymer can achieve efficiencies $>7\%$[12] and are still showing potential to increase this. They are different from the conventional silicon and other inorganic material based cells as they are cheaper and can be fabricated via low-cost solution processing techniques, such as spin coating, brush painting, and spray coating.[4] These solution-processing techniques yield desired thicknesses of a few hundred nanometers and sober efficiencies of 4 to 5%. The wide multipolymer layered architectures of OSCs help execute the processes of photon trapping, generation of electrons and holes, and transport of charges to the respective cathodes and anodes. It was later reported that an effective way to improve polymer solar cell efficiency is to use a tandem structure; with this method, a broader part of the spectrum of solar radiation is used and the thermalization loss of photon energy is minimized. Yang Yang reported power conversion efficiencies of $>10\%$ in tandem solar cells.[13] Recently, Heliatek and Mitsubishi Chemicals have claimed the highest efficiency of 12 (Ref. 14) and 10%,[15] respectively, for OSCs. Another kind of device is dye-sensitized solar cells (DSSCs), which have gained unparalleled growth in recent years due to their ease of fabrication and superior tunable optical properties. Recently, a DSSC with porphyrin sensitizers has achieved a record efficiency of 13% without sacrificing stability.[16]

The key drawbacks, such as efficiency, durability, and stability of OSCs and DSSCs, have made them the least chosen products for commercialization. In 2009, perovskites, a new solar

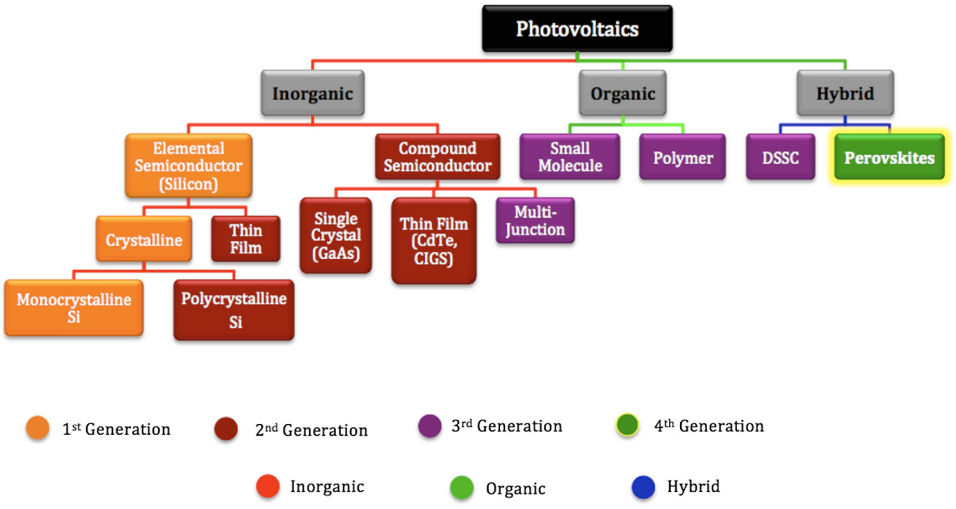

Fig. 1 Basic classification of photovoltaics.

cell material, evolved to transform photovoltaics and currently displays outstanding potential with power conversion efficiencies of 19.7%[17] in the laboratory. Perovskite-based solar cells are purported to have the potential to provide sustainable and efficient power via cost-effective modes and techniques. Several research groups, such as Henry Snaith from Oxford University, Andrew Rappe at University of Pennsylvania, Sang II Seok at South Korean Institute KRICT, Michael Gratzel from EPFL, and Yang Yang from UCLA, are the frontrunners in the efforts to double the efficiency of these materials in less than a year.[18–21] These devices are at the point of maximum optimism and are predicted to reach 50% efficiencies in the near future.[22] These devices are also known for their high photon absorptivity, wide direct band gaps with superior carrier charge transports,[23] and cost-effective modes of fabrication.

2 Significance of Perovskites

Perovskite is a mineral that came into existence when a German mineralogist, Gustav Rose, discovered calcium titanate ($CaTiO_3$) in 1839; it is named after a Russian mineralogist, Lew A. Perovski. Additionally, the compounds having a similar nomenclature to $CaTiO_3$ or the family of materials exhibiting the stoichiometry as ABX_3 are also known as perovskites. This ambiguity of terminology of the structural family and a mineral has been explicitly elucidated by Muller and Roy.[24] They sought to address the ambiguity by proposing that the original mineral composition would be enclosed in square brackets. Thus, [$CaTiO_3$] stands for the perovskite structures and not the composition $CaTiO_3$.

The A, B, and X in the perovskite crystal structure are typically represented as a larger rare earth metal cation, a smaller metal cation, and anions (O^{2-}, Cl^-, Br^-, I^-, or, in a few instances, S^{2-}), respectively, arranged in octahedral symmetry as shown in Fig. 2. In the idealized (cubic) perovskite structure, the large A cations are in 12 coordinates and the smaller B cations occupy octahedral holes formed by the large X anions. There are many different perovskite materials, such as $CaTiO_3$, $MgSiO_3$, $SrFeO_3$, $BaTiO_3$, $LiNbO_3$, $SrZrO_3$, and the nonoxide $KMgF_3$, that, with skilled chemical manipulation, can produce an incredibly wide array of phases with a multitude of functionalities that include dielectric,[25,26] ferroelectric,[27–30] magnetoresistive,[28] thermoelectric,[31] electro-optic,[32] semiconducting,[33] conducting,[28,34] and superconduction.[29,35]

The concept of a two-dimensional layered organic-inorganic perovskite structure was derived from the three-dimensional (3-D) ABX_3 structure by cutting 3-D perovskite into one layer thick slice along the ⟨100⟩ direction.[36] It is known from the first-principles study that the replacement of an inorganic A cation in a basic cubic perovskite structure by a suitable organic cation provides a material of a superior scope with a broad selection of properties.[37] In the early 1990s, an IBM researcher, David B. Mitzi, explored the structure-property relationship in organic-inorganic hybrid perovskite materials by replacing A with a cationic organic molecule, B with an inorganic post-transition metal, and X with halides, such as methylammonium tin iodide

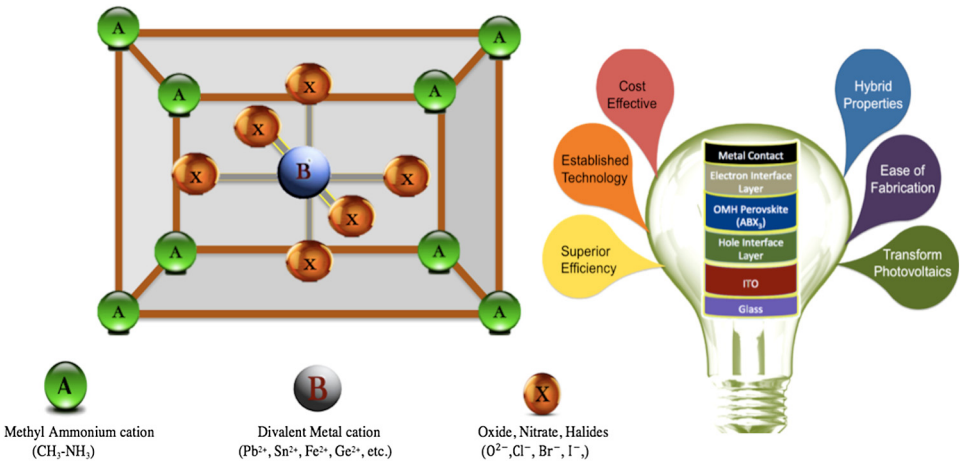

Fig. 2 (a) Typical octahedral structure of pervoskite crystal (ABX_3). (b) Detailed features of perovskite solar devices.

($CH_3NH_3SnI_3$) and methyl ammonium lead iodide ($CH_3NH_3PbI_3$).[29] These organo-metal halide (OMH) perovskite materials are engineered for diverse thin-film devices, such as solar cells,[38,39] thin-film transistors,[40] and light-emitting diodes.[38,40] Strong diffraction peaks are observed at 14.02 deg and 28.3 deg, corresponding to the reflections from (110) and (220) crystal planes of the tetragonal perovskite structure on TiO_2, which is shown in Fig. 3.

The nomenclatures with a methylammonium (CH_3-NH_3^+) organic cation and the inorganic metal halide octahedra's (SnI_2, PbI_2) create a blend of hybrid perovskites with evolving physical, optical, mechanical, and electrical properties. The OMH perovskites have strong intermolecular hydrogen bonds between the amino and halide group ions, whereas the weak Vander Waals exists among the organic ions. The divalent transition metal ions (such as Cu^{2+}, Ni^{2+}, Co^{2+}, Fe^{2+}, Mn^{2+}, Pd^{2+}, Sn^{2+}, Pb^{2+}, etc.) function as the best metal cations for the organic-inorganic framework. Among these combinations, those belonging to group 14 (including Sn^{2+} and Pb^{2+}) attracted more interest due to their good optoelectronic properties and potential for low-temperature device fabrication.[20,34,42] The most predominantly used metal cations Sn^{2+} and Pb^{2+} with melting points of 505 and 600 K, respectively, are generally unreactive, stable at room temperature, and abundant in the Earth's crust. The employment of the least electronegative halide anions improves the perovskite structures for strong absorption over wide band gaps. Additionally, lowering the Pauling electronegativity between the metal cation and halide anion can decrease the band gaps. The replacement of pure halides by mixed halides with changing ratios in the OMH perovskites can enhance the tuning capabilities of optical absorption or produce superior recombination properties.[36] Therefore, the OMH structures such as $AB(Br_xI_{1-x})_{3-y}Cl_y$ are evolved.

The geometrical size and structure of the organic cation is critical to make a best fit in the relatively small cuboctahedral hole, therefore, the A cation in the perovskite structure is limited to the smallest organic molecules, such as methylammonium ion ($CH_3NH_3^+$). However, this decrease in the A cation's size has to be optimized by tightening the contact with anions in the cubic structure. This phenomenon of shrinking the geometrical constraints tends to distort the octahedral BX_6 structure and introduces a distortion factor, also known as Goldschmidt's tolerance factor.[43] This is named after a Norwegian mineralogist, Viktor Moritz Goldschmidt, who studied a wide range of perovskite crystals and also helped to lay the foundation for the science of crystal chemistry. Typically, a Goldschmidt's tolerance factor (t) of less than unity makes a suitable perovskite structure and is described as[44]

$$t = \frac{(R_A + R_X)}{\sqrt{2}(R_B + R_X)}, \tag{1}$$

where R_A, R_B, and R_X are the corresponding ionic radii of A, B, and X. For example, the larger organic methylammonium cation replaces A with an ionic radius of ($R_A = 1.87$ Å);[45] B with the most capable metal cation Pb^{2+} ($R_B = 1.19$ Å) and Sn^{2+} ($R_B = 0.93$ Å); and the X anion with

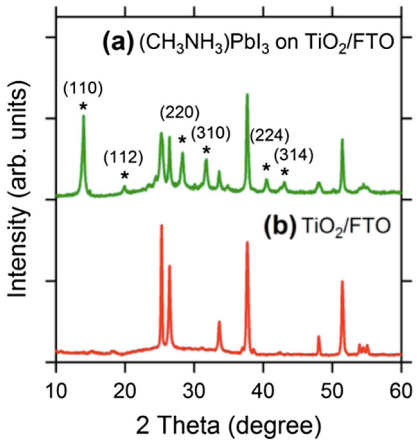

Fig. 3 X-ray diffraction peaks spectra of (a) $CH_3NH_3PbI_3$ on TiO_2 and (b) as-grown mesoporous TiO_2. Reprinted with permission from Ref. 41.

the uniquely distinguished halide ions Cl^- ($R_X = 1.81$ Å), Br^- ($R_X = 1.96$ Å), and I^- ($R_X = 2.2$ Å). It is evident from the above geometries that the lead halide perovskites ($0.84 < t < 0.86$) have higher tolerations than their tin ($0.91 < t < 0.95$) counterparts; hence, the superior properties of lead over tin perovskites is demonstrated and the use of lead is justified.

3 Atomistic Origin and Charge Transport Mechanism in OMH Perovskites

In the diverse field of solar cells, the selection of materials of merit is critical and, in some cases, is presented as a trade-off factor among durability, stability, cost, ease of fabrication, and efficiency. An ideal solar cell material requires inheriting properties such as stronger and broader absorptions, ultrafast carrier charges separation and transport, high dielectric, and optimized diffusion lengths so that swift recombination occurs. By extending its organic and inorganic features to the bottlenecked efficiencies of organic PVs, the 3-D framework of methylammonium metal halide perovskite becomes an important modern scientific breakthrough. Typical absorption spectra of perovskite devices and its normalized spectra as a function of TiO_2 thickness are shown in Fig. 4.

In 2009, Miyasaka et al. published a report on using OMH perovksites as visible light sensitizers yielding efficiencies of 3.81%, where it interacts with the conduction band levels of TiO_2.[39] Further investigations on these class of materials have revealed that they can augment the efficiencies and are exceptional to low electron and hole transport lengths, which are predominant among low-temperature solution-processed PV.[21,46–48]

3.1 *Dielectric Behavior*

The compelling ferroelectric properties of 3-D structured OMH perovskites can be explained by the polar nature of methylammonium salt (CH_3-NH_3^+) with a permanent dipole moment, and the structural distortions carried by the lone pairs of lead ($6s^2$) and tin ($5s^2$). These cubic superlattices consisting of semiconductor metal iodide layers sandwiched between insulator methylammonium layers can easily change their orientation and, thus, create the octahedral dielectric confinement of excitons.[49] Typically, the excitons in organic molecules observe the Frenkel-Peierls model, leading to stronger bonds between them, higher exciton binding energies, and the least Bohr radius. These characteristics, consequently, tend to lower the dielectric constants and contribute to a poor charge transport in the conventional organic PV. On the contrary, the excitons in OMH perovskites exhibit the Wannier-Mott model[30,50] due to their organic and inorganic behaviors. In these materials, the excitons experience the least binding energies and higher

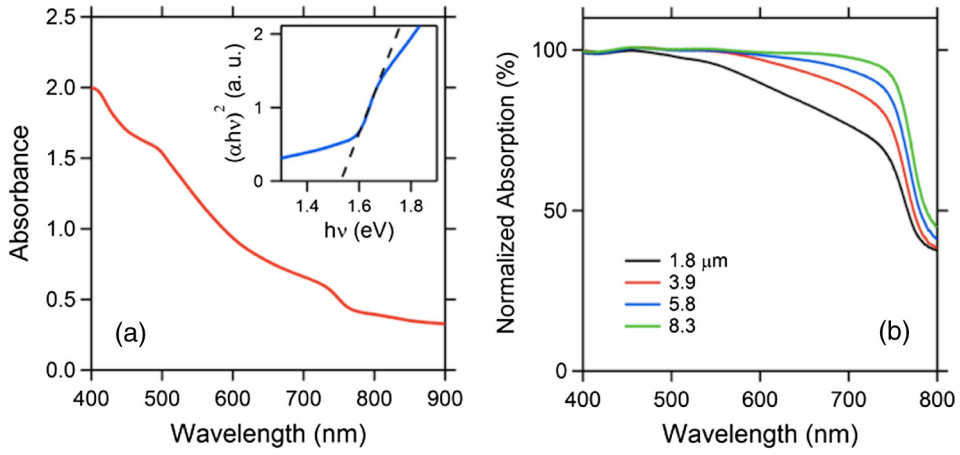

Fig. 4 UV-Vis absorption spectra of (a) $CH_3NH_3PbI_3$ on TiO_2 and (b) normalized absoprtion as a function of TiO_2 thickness. Reprinted with permission from Ref. 41.

Bohr's excitonic radius, thereby yielding superior charge transports. The exciton-evaluating components can be described by the well-known equations of binding energy (E_b) and the Bohr radius (r_B) of the excitons,

$$E_b = 13.6\frac{\mu}{\varepsilon^2}\ (\text{eV}), \tag{2}$$

$$r_B = 0.529\frac{\varepsilon}{\mu}\ (\text{A}^0), \tag{3}$$

where ε is the dielectric permittivity and μ is the exciton pair mass. Table 1 presents the trends in dielectric constants for various halides. However, the strong inherited polarization due to the ionic compounds (which have permanent dipole moment), the presence of an inorganic anion, and an organic cation yields higher dielectric constants, thus exhibiting a smooth mechanism for good long-range charge transport via band structure or polaron hopping.[35] Table 1 details the dielectric and exciton behaviors in OMH perovskites.

3.2 *Charge Transport*

The charge transport in OMH perovskite solar cells mostly resembles the conventional DSSCs. Zhao and Zhu report that the intensity-modulated photocurrent or photovoltage spectroscopies show that the transport and recombination properties of solid-state mesostructured perovskite solar cells are similar to those of solid-state DSSCs.[41] They also report that the electron diffusion length decreases from 16.9 to 5.5 μm as the TiO_2 film thickness increases from 1.8 to 8.3 μm, revealing that the light absorption increases with an increasing TiO_2 film thickness, thereby allowing for faster recombination which limits the solar conversion process.

Recently, Wehrenfennig et al. concluded that the OMH perovskites allow for an unexpected combination of both low charge recombination rates and high charge-carrier mobilities and are, therefore, the best candidates for light absorption and charge transport in solar cells.[56] It is necessary to further explore the charge transports and electronic structures of OMH perovskite materials. The relativistic GW (Green's function and Wick's theorem of density functional theory) calculations on the electronic and optical properties predict $MASnI_3$ to be a better electron transporter than $MAPbI_3$.[57] It is evident from Fig. 5 that the resistivity versus temperature of lead- and tin-based perovskites is similar to the characteristics of undoped semiconductor and displays a perfect ohmic behavior.[33]

However, these OMH perovskite materials act as light sensitizers and ambipolar electron and hole transport materials,[58] or they absorb light, thus creating the excitons (electron-hole pair). This involves steps like (1) creation of electron-hole pairs upon absorption of light by the perovskite; (2) formation of excitons after thermalization of the carriers; (3) charge separations at the junctions of electron and hole transport layers (HTLs); (4) injection of holes and electrons into the respective transport layers, such as spiro-2,2',7,7'-tetrakis-(N,N-di-p-methoxyphenylamine)9,9'-spirobifluorene (OMeTAD) and TiO_2; (5) extraction of those charge carriers to the external circuit by contacts. Thus, it is vital to understand the OMH perovskite material stoichiometry and cell architecture to arrive at the best cell performance. So far, two types

Table 1 Dielectric and optical parameters of organo-metal halide (OMH) perovskites.

OMH	Crystal structure	Color	Dielectric constant	Optical band gap	Bohr radius (r_B)	Exciton binding energy (E_b)
$MAPbI_3$	Cubic (330.4 K)[51] Tetragonal (161.4 K) Orthorhombic (161.4 K)	Black	28.8 (Ref. 45)	1.63 eV (Ref. 52)	22 Å	37 meV (Ref. 53)
$MAPbBr_3$	Cubic (236.3 K)[51] Tetragonal (154 K) Orthorhombic (148.8 K)	Yellowish orange	25.5 (Ref. 45)	2.32 eV (Ref. 54)	20 Å	76 meV
$MAPbCl_3$	Cubic (177.2 K)[51] Tetragonal (171.4 K) Orthorhombic (171.4 K)	Colorless	23.9 (Ref. 45)	3.11 eV (Ref. 55)	17 Å	100 meV

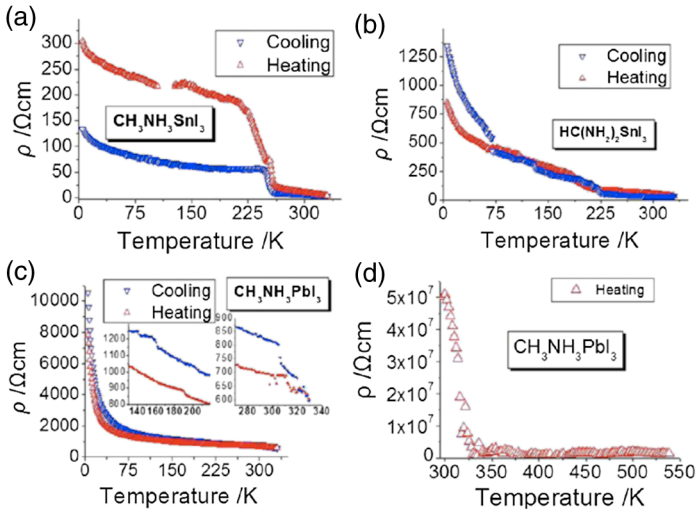

Fig. 5 The temperature-dependent resistivity plots of lead- and tin-based perovskite single crystals. Reprinted with permission from Ref. 33.

of device architectures, namely mesostructured and planar heterojunction, have been adapted. Figure 6 describes the band structure of a typical perovskite solar cell. The first mesostructure is derived from the conventional solid-state DSSCs, and in the latter, the perovskite layer is sandwiched between the electron (TiO_2, Al_2O_3, etc.) and hole [poly(3-hexylthiopene-2,5-diyl (P3HT), spiro-OMeTAD, etc.] transport layers. Figure 7(a) displays the typical cross-sectional SEM image of mesostructured architecture of perovskite solar cells and reveals that the pores of the mp-TiO_2 film are infiltrated with $CH_3NH_3PbI_3$ perovskite. The surface SEM image in Fig. 7 (b) is crucial for determining the filling fraction and infiltration depth of $CH_3NH_3PbI_3$ and HTL into mp-TiO_2. The transparent conducting oxide films, such as indium tin oxide (ITO) and fluorine-doped tin oxide (FTO), are widely used as electrodes due to their striking features such as low electrical resistance, high optical transmittance, and high photoconductivity.[59] However, ITO and FTO are limited by the infrared wavelengths; in particular, the ITO-based substrates have low thermal stability, which explains the high efficiencies produced by FTOs.

The mechanism of conduction depends largely on charge-carrier diffusion length, which generally means a thicker absorber layer for greater light trapping and is considered one of the key parameters of solar cell performance. After photoexcitation, the electron-hole pairs generated are dissociated in a few picoseconds (~2 ps). The presence of metal oxide TiO_2 with a high electron affinity accelerates the formation of charges and motivates efficient electron injection for <1 ps. The faster electron injection in $CH_3NH_3PbI_3/TiO_2$ is supported by the terahertz (THz) photoconductivity transient kinetic studies with normalized excitation density, which shows that the charge mobility of $CH_3NH_3PbI_3/TiO_2$ (~7.5 $cm^2/V \cdot s$) is three to four times lower than that in neat $CH_3NH_3PbI_3$ and $CH_3NH_3PbI_3/Al_2O_3$ (~20 $cm^2/V \cdot s$).[61] However, the unbalanced transport of charges resulting in space charge limited photocurrents and a lowering of the power

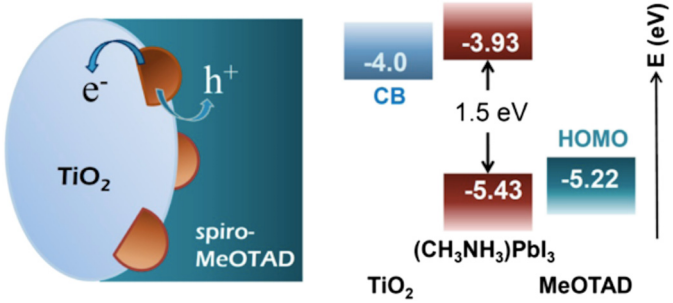

Fig. 6 Energy band levels of $TiO_2/CH_3NH_3PbI_3$/spiro-OMeTAD showing the conduction and valence bands. Reprinted with permission from Ref. 48.

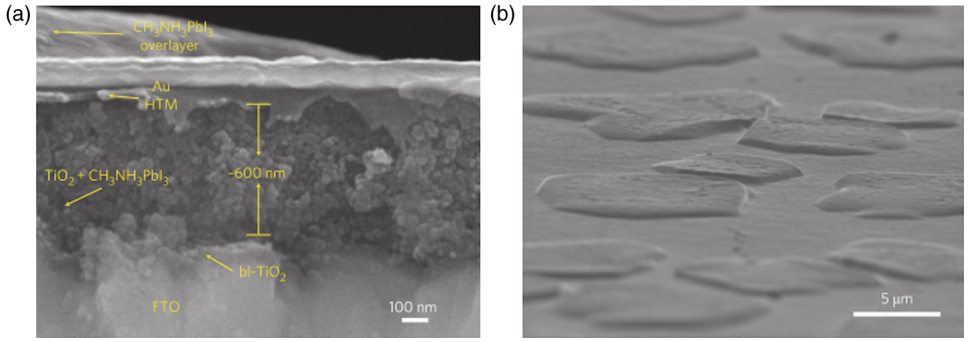

Fig. 7 (a) Cross-sectional SEM image of organo-metal halide (OMH) perovskite. (b) Surface SEM image of $CH_3NH_3PbI_3$ on TiO_2. Reprinted with permission from Ref. 60.

conversion efficiency (PCE) can be attributed to the low intrinsic mobility of TiO_2.[62] A few other research groups have reported higher efficiencies of 15.7% with Al_2O_3 layers[63] and 4.2% with ZrO_2 buffer layer,[58] respectively.

The THz photoconductivity spectra of pristine OMH perovskite shown in Fig. 8 compares its composition with TiO_2 and Al_2O_3. Slow electron–hole recombination and persistent high mobility are essential features for an efficient solar cell. The THz response along with other methods concluded that the THz mobilities of electrons are twice as mobile as the holes in the perovskite phase.[61]

The degradation of OMH perovskites with humidity, ambient light, and oxidation can be attributed to the strong absorption onset of the material shifting from 1.6 to 2.4 eV. This low Urbach energy measured for perovskites can be a strong indicator that this material will not suffer from the Staebler–Wronski effect.[64] The degradation of the cell performance is normally accompanied by a color bleaching of perovskites even when the cells are stored in the dark, suggesting that the chemical instability of perovskites in the iodide electrolyte contributes to the degradation of the cell performance over time. The exact degradation mechanism is still unknown, and it is crucial to know to what extent the material changes when measured at an ambient atmosphere or when exposed to liquid electrolytes. Therefore, a number of detailed degradation studies are required to further explore its usage for photoelectrochemical applications in the future.

The OMH perovskite layer, typically with thicknesses of ~100 to 200 nm, determines the exciton diffusion lengths (L_d) and their lifetimes (τ), unlike the OSCs with a larger L_d than these ($CH_3NH_3PbI_3$) materials (5 to 10 nm), and yields extended exciton lifetimes of >50 ns (Ref. 65)

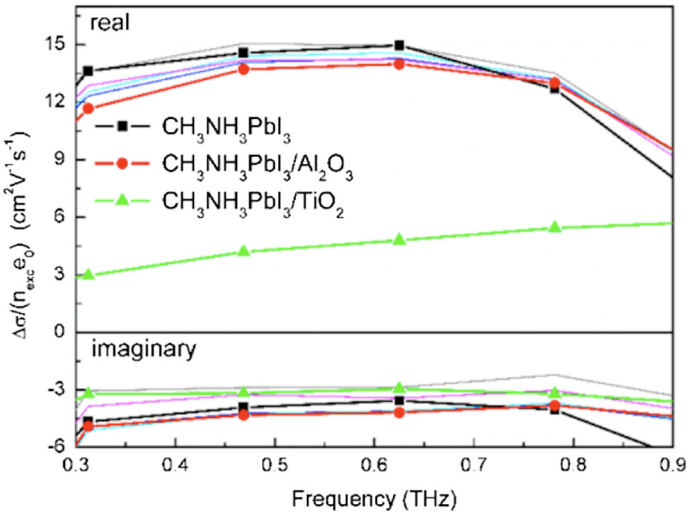

Fig. 8 Terahertz photoconductivity spectra of $TiO_2/CH_3NH_3PbI_3$ and $Al_2O_3/CH_3NH_3PbI_3$ at different pump probe delays. Reprinted with permission from Ref. 61.

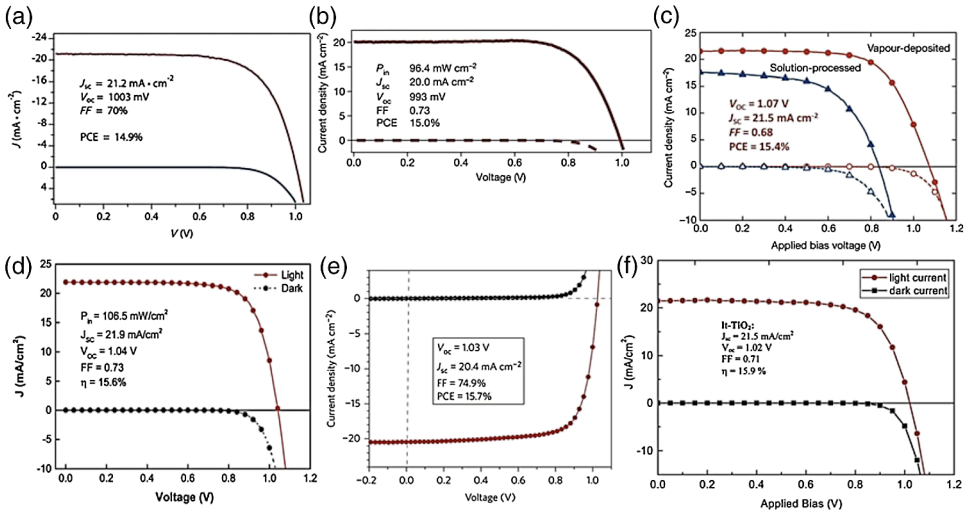

Fig. 9 J–V curves of various OMH perovskite devices: (a) $TiO_2/CH_3NH_3PbI_3$/spiro-OMeTAD, (b) $TiO_2/CH_3NH_3PbI_3$/spiro-OMeTAD, (c) $TiO_2/CH_3NH_3PbI_{3-X}Cl_X$/spiro-OMeTAD, (d) graphene-TiO_2/meso-$Al_2O_3/CH_3NH_3PbI_{3-X}Cl_X$/spiro-OMeTAD, (e) $ZnO/CH_3NH_3PbI_3$/spiro-OMeTAD, (f) $TiO_2/CH_3NH_3PbI_{3-X}Cl_X$/spiro-OMeTAD. Reproduced with permission from Ref. 20.

when compared to 8 ns of OSC,[66] motivating them to travel to the contacts before decay. Various research groups have investigated different halides (Cl, Br, and I),[51,67,68] and mixed halides, such as $CH_3NH_3PbI_2Cl$, $CH_3NH_3PbI_2Br$, or vice versa.[38,50,63,69] However, the destructive effects of lead (Pb) brands tin (Sn) as a more suitable potential candidate for the perovskite structure. Mitzi investigated its ($CH_3NH_3SnI_3$) applicability for tuning the band gap, which was later introduced by various others[31,33,34,36,38] as a key feature of conducting photovoltaics. A maximum PCE of 12.3% was achieved with $CH_3NH_3PbI_2Br$. It is evident from Table 1 that the optical band gaps and exciton binding energies follow a trend, indicating the tunability and application-specific functionalities. However, a detailed study in different mixed halide materials is required to determine the electronic and optical properties.

Typically, the perovskite solar cells suffer from high series and shunt resistance, thereby yielding poor fill factor values. This can be attributed to the higher conductivity of the perovskite layer being surpassed by the thicker layer of the lower conductive hole transport material (HTM) layer. Therefore, a thinner and better conductive HTM layer that enhances the hole mobility is highly desired for these devices. Bi et al. reported PCEs of 8.5, 4.5, and 1.6% by incorporating various HTMs, such as spiro-OMeTAD, P3HT, and 4-(diethylamino)-benzaldehyde diphenylhydrazone, respectively.[70] Eventually, spiro-OMeTAD caught the attention of researchers and it was discovered that doping a lithium salt lithilum bis-trifluoromethanesulfonimide (Li-TFSI) can increase hole conductivity.[71] The spectroscopy studies later revealed that the Fermi level in spiro-OMeTAD shifts toward the HOMO, and 24% of the spiro-OMeTAD molecules get oxidized in presence of Li-TFSI.[72] Spiro-OMeTAD as a superior HTM layer is widely used to improve the device performance through enhancing its conductivity, as they mainly functioned to increase the hole mobility and charge density of HTMs, respectively, or increase both simultaneously.[73] Figure 9 shows the J–V curves for various perovskite devices with mixed and pure compositions.

4 Fabrication Procedures

The fabrication methodologies technically drive the performance and efficiency of perovskite solar cells, so it is vital to deposit the light sensitizer OMH perovskite material to enhance the device kinetics. The thinner cells tend to poorly absorb light, whereas in thicker cells, the charge carriers cannot travel through to reach the contacts.[74] Despite their higher performance, they degrade at a faster rate, which is normally accompanied by a color bleaching due to the chemical instability of perovskites in the iodide electrolyte.[41] Figure 10(a) showcases a multitude of

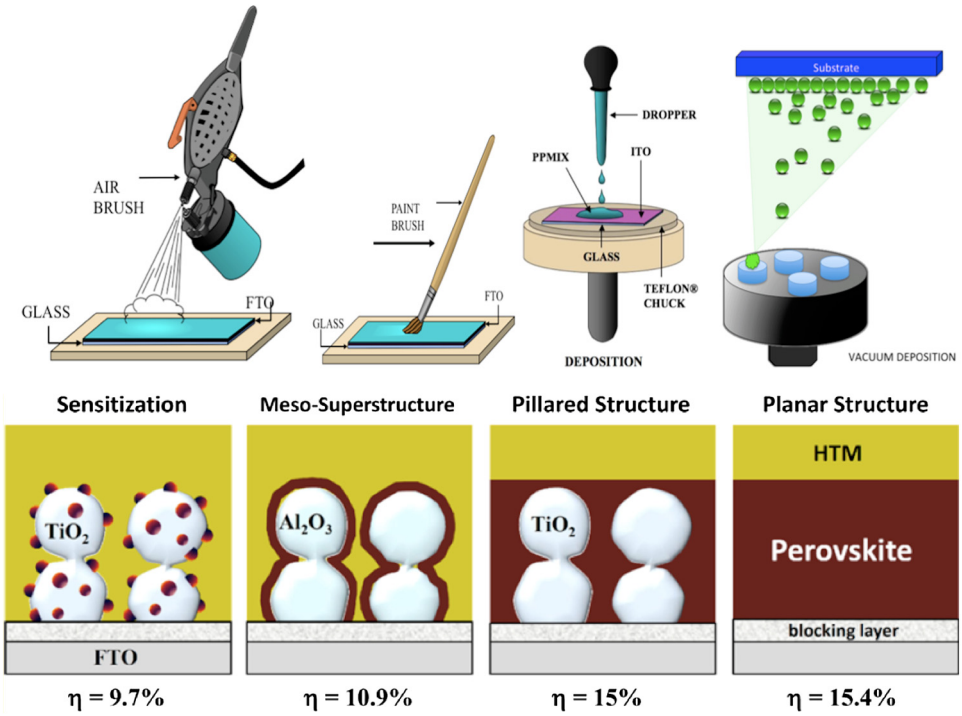

Fig. 10 (a) Fabrication methods adopted for perovskite solar cells. (b) Architectures of typical perovskite solar cells. Reprinted with permission from Ref. 35.

techniques, such as solution processing, and deposition that can be demonstrated for the fabrication of perovskite-based solar cells.

The ability to deposit these hybrid perovskites is very crucial to sustain their unique properties. So far, many researchers have determined the best fabrication procedures to be solution-processed techniques, evaporation, sequential deposition, and other techniques. Although the handiness of solution processing is widely encouraged, its drawbacks, such as poor wetting and inconsistency of hybrid materials, class them as a hindrance for an efficient solar device. An IBM researcher, Mitzi, has developed a novel melt processing technique for these hybrid films on flexible substrates.[75] A few researchers crafted a unique low temperature processing technique that incorporates an Al_2O_3 scaffold in a perovskite material.[76] Figure 10(b) illustrates various architectures investigated and efficiencies achieved for hybrid perovskite solar cells. A few researchers reported that increasing the conductivity of the HTMs by doping and optimizing charge collection by adjusting the absorber thickness could bring a positive impact on PCEs in planar heterojunction-based solar cells.[73] The devices with longer diffusion lengths (1000 nm)[77–79] are more efficient; therefore, the thicknesses and morphology of every functional layer is vital to drive the device to superior efficiencies. Edri et al. explained that the electrons could transport across only a short shallow barrier, whereas a hole can travel a long distance before recombining, thus clearly indicating that the $CH_3NH_3PbI_3$ makes an efficient solar cell (15%) with mesoporous TiO_2 scaffolds.[54] Flexible devices on ITO/polyethylene terephthalate substrates can also be prepared by this route and display PCEs in excess of 10%.

The combination of ease-of-fabrication, room-temperature processing, high device performance, and device flexibility are all expected to help enhance the most needed PV characteristics, such as efficient carrier collection and/or exciton dissociation, improved mobility within the electron transport layer, and extensive light scattering for these hybrid organic-inorganic solar devices.

5 Future Outlook

The usage of lead in perovskites deteriorates its culture for commercial applications, therefore, an exploratory drive to replace it with other divalent and least toxic metals, such as tin, copper,

germanium, manganese, or iron, can change the dynamics of perovskite solar cells; current research is trending along these lines. The scientific community anticipates that these particular devices will make a successful entry to the commercial market by 2020. Further, exploration of superior materials that can tune ferroelectric domains and provide rapid support to the excitonic reactions in perovskite crystals can yield a better class of devices with the best durability and degradability.

The recent advent of nanotechnology makes it worthwhile to investigate the role of nano-perovskites to enrich the performance and efficiency of any device. Additionally, the device cost can revolutionize the current photovoltaic technology, which is possible by developing more bench-top processes, such as printing, spraying, etc., rather than the clean room and high-tech equipment. Hence, there is a great need and urgency to develop an easy methodology of fabricating these devices. Some researchers believe that it can resemble the single crystal silicon and an OMH perovskite single crystal grown by melt-process or gel method will be eventually be a reality. Finally, its high transparency (>825 nm) is a predictor of superior functionalities by integrating these exotic devices in a tandem architecture.

Acknowledgments

The authors acknowledge the DHS-BS and NSF-EPSCoR program and summer research program facilitated by Oak Ridge National Laboratory's HBCU/MEI program.

References

1. S. Kazim et al., "Perovskite as light harvester: a game changer in photovoltaics," *Angew. Chem. Int. Ed. Engl.* **53**(11), 2812–2824 (2014).
2. P. Frankl, "Technology roadmap: solar photovoltaic energy," 11 May 2010, http://www.iea.org/publications/freepublications/publication/technology-roadmap-solar-photovoltaic-energy---foldout.html (18 November 2014).
3. S. A. Kalogirou, "Solar thermal collectors and applications," *Prog. Energy Combust. Sci.* **30**(3), 231–295 (2004).
4. A. K. Chilvery et al., "A versatile technique for the fabrication of PEDOT: PSS films for organic solar cells," *Energy, Sci. Technol.* **4**(2), 6–11 (2012).
5. S.-S. Sun and N. S. Sariciftci, *Organic Photovoltaics*, p. 640, CRC Press, T&F Group, London (2005).
6. NREL Cell Efficiencies, "efficiency_chart" (2012).
7. M. A. Green, "Crystalline and thin-film silicon solar cells: state of the art and future potential," *Sol. Energy* **74**(3), 181–192 (2003).
8. M. A. Green et al., "Solar cell efficiency tables," *Prog. Photovolt. Res. Appl.* **20**, 12–20 (2012).
9. H. Shirakawa et al., "Synthesis of electrically conducting organic polymers: halogen derivatives of polyacetylene, (CH) x," *J. Chem. Soc. Chem. Commun.* **16**, 578 (1977).
10. M. Pagliaro, R. Ciriminna, and G. Palmisano, "Flexible solar cells," *ChemSusChem* **1**(11), 880–891 (2008).
11. A. C. Mayer et al., "Polymer-based solar cells," *Mater. Today* **10**(11), 28–33 (2007).
12. G. Li, R. Zhu, and Y. Yang, "Polymer solar cells," *Nat. Photonics* **6**, 153–161 (2012).
13. J. You et al., "A polymer tandem solar cell with 10.6% power conversion efficiency," *Nat. Commun.* **4**, 1446 (2013).
14. Heliatek, "Heliatek press release," 2013, http://www.heliatek.com/?lang=en (18 November 2014).
15. M. C. Scharber and N. S. Sariciftci, "Efficiency of bulk-heterojunction organic solar cells," *Prog. Polym. Sci.* **38**(12), 1929–1940 (2013).
16. P. Simon et al., "Dye-sensitized solar cells with 13% efficiency achieved through the molecular engineering of porphyrin sensitizers," *Nat. Chem.* **6**, 242–247 (2014).
17. H. Zhou et al., "Interface engineering of highly efficient perovskite solar cells," *Science* **345**(6196), 542–546 (2014).

18. M. Liu, M. B. Johnston, and H. J. Snaith, "Efficient planar heterojunction perovskite solar cells by vapour deposition," *Nature* **501**(7467), 395–398 (2013).
19. I. Grinberg et al., "Perovskite oxides for visible-light-absorbing ferroelectric and photovoltaic materials," *Nature* **503**(7477), 509–517 (2013).
20. P. Gao, M. Grätzel, and M. K. Nazeeruddin, "Organohalide lead perovskites for photovoltaic applications," *Energy Environ. Sci.* **7**(8), 2448–2463 (2014).
21. J. You et al., "Perovskite solar cells with high efficiency and flexibility," *ACS Nano* **8**(2), 1674–1680 (2014).
22. B. Bulkin, "Perovskites: the future of solar power?," in *Guardian*, p. 1, http://www.theguardian.com/sustainable-business/perovskites-future-solar-power (18 November 2014).
23. H. J. Snaith, "Perovskites: the emergence of a new era for low-cost, high-efficiency solar cells," *J. Phys. Chem. Lett.* **4**, 3623–3630 (2013).
24. O. Muller and R. Roy, "The major ternary structural families," in *Cryst. Chem. Non-Metallic Mater.*, Springer-Verlag, Berlin, Heidelbergle (1974).
25. E. J. Juarez-Perez et al., "Photoinduced giant dielectric constant in lead halide perovskite solar cells," *J. Phys. Chem. Lett.* **5**(13), 2390–2394 (2014).
26. A. K. Batra et al., "Simulation of energy harvesting from roads via pyroelectricity," *J. Photonics Energy* **1**(1), 014001 (2011).
27. A. A. Bokov and Z. G. Ye, "Recent progress in relaxor ferroelectrics with perovskite structure," *J. Mater. Sci.* **41**(1), 31–52 (2006).
28. M. A. Loi and J. C. Hummelen, "Hybrid solar cells: perovskites under the Sun," *Nat. Mater.* **12**(12), 1087–1089 (2013).
29. D. B. Mitzi, "Synthesis, structure, and properties of organic-inorganic perovskites and related materials," in *Progress in Inorganic Chemistry*, K. D. Karlin, Ed., p. 121, John Wiley & Sons, West Sussex, England, New York (1999).
30. J. M. Frost et al., "Atomistic origins of high-performance in hybrid halide perovskite solar cells," *Nano Lett.* **14**(5), 2584–2590 (2014).
31. Y. Takahashi et al., "Charge transport in tin-iodide perovskite: origin of high conductivity," *Dalt. Trans.* **40**(20), 5563–5568 (2011).
32. A. Bhalla, R. Guo, and R. Roy, "The perovskite structure—a review of its role in ceramic science and technology," *Mater. Res. Innov.* **4**(1), 3–26 (2000).
33. C. C. Stoumpos, C. D. Malliakas, and M. G. Kanatzidis, "Semiconducting tin and lead iodide perovskites with organic cations: phase transitions, high mobilities, and near-infrared photoluminescent properties," *Inorg. Chem.* **52**(15), 9019–9038 (2013).
34. D. B. Mitzi et al., "Conducting tin halides with a layered organic-based perovskite structure," *Nature* **369**, 467–469 (1994).
35. H.-S. Kim, S. H. Im, and N.-G. Park, "Organolead halide perovskite: new horizons in solar cell research," *J. Phys. Chem. C* **118**(11), 5615–5625 (2014).
36. J. L. Knutson, J. D. Martin, and D. B. Mitzi, "Tuning the band gap in hybrid tin iodide perovskite semiconductors using structural templating," *Inorg. Chem.* **44**(13), 4699–4705 (2005).
37. R. S. Roth, "Classification of perovskite and other AB03 type compounds," *J. Res. Natl. Bur. Stand. (1934).* **58**(2), 75–88 (1957).
38. D. B. Mitzi, "Templating and structural engineering in organic-inorganic perovskites," *J. Chem. Soc. Dalt. Trans.* **1**(1), 1–12 (2001).
39. A. Kojima et al., "Organometal halide perovskites as visible-light sensitizers for photovoltaic cells," *J. Am. Chem. Soc.* **131**(17), 6050–6051 (2009).
40. D. B. Mitzi, K. Chondroudis, and C. R. Kagan, "Organic-inorganic electronics," *IBM J. Res. Dev.* **45**(1), 29–45 (2001).
41. Y. Zhao and K. Zhu, "Charge transport and recombination in perovskite (CH_3NH_3) PbI_3 sensitized TiO_2 solar cells," *J. Phys. Chem. Lett.* **4**, 2880–2884 (2013).
42. I. B. Koutselas, L. Ducasse, and G. C. Papavassiliou, "Electronic properties of three- and low-dimensional semiconducting materials with Pb halide and Sn halide units," *J. Phys. Condens. Matter* **8**, 1217–1227 (1996).
43. X. W. Zhou, F. P. Doty, and P. Yang, "Atomistic models for scintillatory discovery," *Proc. SPIE* **7806**, 78060E (2010).

44. V. M. Goldschmidt, "Geochemisce Verterlungsgesetze der Elemente," in *Nor. Videnskap, Oslo*, I kommission hos J. Dybwad, Oslo (1927).
45. A. Poglitsch and D. Weber, "Dynamic disorder in methylammoniumtrihalogenoplumbates (II) observed by millimeter-wave spectroscopy," *J. Chem. Phys.* **87**(11), 6373 (1987).
46. G. Xing et al., "Long-range balanced electron- and hole-transport lengths in organic-inorganic CH3NH3PbI3," *Science* **342**(6156), 344–347 (2013).
47. H. J. Snaith, "Estimating the maximum attainable efficiency in dye-sensitized solar cells," *Adv. Funct. Mater.* **20**(1), 13–19 (2010).
48. N. Park, "Organometal perovskite light absorbers toward a 20% efficiency low-cost solid-state mesoscopic solar cell," *J. Phys. Chem. Lett.* **4**, 2423–2429 (2013).
49. N. A. Gippius et al., "Dielectrically confined excitons and polaritons in natural superlattices —perovskite lead iodide semiconductors," *J. Phys. IV* **3**, 437–440 (1993).
50. S. a. Bretschneider et al., "Research update: physical and electrical characteristics of lead halide perovskites for solar cell applications," *APL Mater.* **2**(4), 040701 (2014).
51. H. Mashiyama and Y. Kurihara, "Disordered cubic perovskite structure of $CH_3NH_3PbX_3$ (X = Cl, Br, I)," *J. Korean Phys. Soc.* **32**, 156–158 (1998).
52. Z. Chen et al., "Shape-controlled synthesis of organolead halide perovskite nanocrystals and their tunable optical absorption," *Mater. Res. Express* **1**(1), 015034 (2014).
53. B. Conings et al., "Perovskite-based hybrid solar cells exceeding 10% efficiency with high reproducibility using a thin film sandwich approach," *Adv. Mater.* **26**(13), 2041–2046 (2014).
54. E. Edri et al., "High open-circuit voltage solar cells based on organic-inorganic lead bromide perovskite," *J. Phys. Chem. Lett.* **4**(6), 897–902 (2013).
55. N. Kitazawa, Y. Watanabe, and Y. Nakamura, "Optical properties of $CH_3NH_3PbX_3$ (X = halogen) and their mixed-halide crystals," *J. Mater. Sci.* **37**, 3585–3587 (2002).
56. C. Wehrenfennig et al., "High charge carrier mobilities and lifetimes in organolead trihalide perovskites," *Adv. Mater.* **26**(10), 1584–1589 (2014).
57. P. Umari, E. Mosconi, and F. De Angelis, "Relativistic GW calculations on $CH_3NH_3PbI_3$ and $CH_3NH_3SnI_3$ perovskites for solar cell applications," *Sci. Rep.* **4**, 4467 (2014).
58. H.-S. Kim et al., "Mechanism of carrier accumulation in perovskite thin-absorber solar cells," *Nat. Commun.* **4**, 2242 (2013).
59. D.-J. Kwak et al., "Comparison of transparent conductive indium tin oxide, titanium-doped indium oxide, and fluorine-doped tin oxide films for dye-sensitized solar cell application," *J. Electr. Eng. Technol.* **6**(5), 684–687 (2011).
60. J. H. Heo et al., "Efficient inorganic-organic hybrid heterojunction solar cells containing perovskite compound and polymeric hole conductors," *Nat. Photonics* **7**(June), 486–491 (2013).
61. C. S. Ponseca et al., "Organometal halide perovskite solar cell materials rationalized: ultrafast charge generation, high and microsecond-long balanced mobilities, and slow recombination," *J. Am. Chem. Soc.* **136**(14), 5189–5192 (2014).
62. E. Hendry et al., "Local field effects on electron transport in nanostructured TiO_2 revealed by terahertz spectroscopy," *Nano Lett.* **6**, 755–759 (2006).
63. M. M. Lee et al., "Efficient hybrid solar cells based on meso-superstructured organometal halide perovskites," *Science* **338**(6107), 643–647 (2012).
64. S. De Wolf et al., "Organometallic halide perovskites: sharp optical absorption edge and its relation to photovoltaic performance," *J. Phys. Chem. Lett.* **5**(6), 1035–1039 (2014).
65. H.-S. Kim et al., "Lead iodide perovskite sensitized all-solid-state submicron thin film mesoscopic solar cell with efficiency exceeding 9%," *Sci. Rep.* **2**, 591 (2012).
66. R. L. Headrick et al., "Anisotropic mobility in large grain size solution processed organic semiconductor thin films," *Appl. Phys. Lett.* **92**(6), 063302 (2008).
67. B. Suarez et al., "Recombination study of combined halides (Cl, Br, I) perovskite solar cells," *J. Phys. Chem. Lett.* **5**(10), 1628–1635 (2014).
68. M. Meister, "Charge generation and recombination in hybrid organic / inorganic solar cells," p. 250, PhD Thesis, Johannes Gutenberg-University Mainz (2013).

69. K. Liang, D. B. Mitzi, and M. T. Prikas, "Synthesis and characterization of organic—inorganic perovskite thin films prepared using a versatile two-step dipping technique," *Chem. Mater.* **10**(1), 403–411 (1998).
70. D. Bi et al., "Using a two-step deposition technique to prepare perovskite ($CH_3NH_3PbI_3$) for thin film solar cells based on ZrO_2 and TiO_2 mesostructures," *RSC Adv.* **3**, 18762–18766 (2013).
71. H. Snaith and M. Gratzel, "Enhanced charge mobility in a molecular hole transporter via addition of redox inactive ionic dopant: implication to dye-sensitized solar cells," *Appl. Phys. Lett.* **89**, 262114 (2006).
72. R. Scholin et al., "Energy level shifts in spiro-OMeTAD molecular thin films when adding Li-TFSI," *J. Phys. Chem.* **116**, 26300–26305 (2012).
73. F. Liu et al., "Numerical simulation: toward the design of high-efficiency planar perovskite solar cells," *Appl. Phys. Lett.* **104**(25), 253508 (2014).
74. G. Xing et al., "Long-range balanced electron- and hole-transport lengths in organic-inorganic $CH_3NH_3PbI_3$," *Science* **342**(6156), 344–347 (2013).
75. D. B. Mitzi, D. R. Medeiros, and P. W. Dehaven, "Low-temperature melt processing of organic-inorganic hybrid films," *Chem. Mater.* **14**(7), 2839–2841 (2002).
76. M. Carnie et al., "A one-step low temperature processing route for organolead halide perovskite solar cells," *Chem. Commun.* **49**, 7893–7895 (2013).
77. Y. Zhao, A. M. Nardes, and K. Zhu, "Solid-state mesostructured perovskite $CH_3NH_3PbI_3$ solar cells: charge transport, recombination, and diffusion length," *J. Phys. Chem. Lett.* **5**, 490–494 (2014).
78. V. Gonzalez-Pedro et al., "General working principles of $CH_3NH_3PbX_3$ perovskite solar cells," *Nano Lett.* **14**(2), 888–893 (2014).
79. L. Barnea-nehoshtan et al., "Surface photovoltage spectroscopy study of organo-lead perovskite solar cells," *Phys. Chem. Lett.* **5**, 2408–2413 (2014).

Biographies of the authors are not available.